

UNCLASSIFIED

AD NUMBER

ADA800091

CLASSIFICATION CHANGES

TO: unclassified

FROM: confidential

LIMITATION CHANGES

TO:
Approved for public release, distribution unlimited

FROM:
Controlling DoD Organization: Wright Air Development Center, Wright-Patterson AFB, OH 45433.

AUTHORITY

WADC/WCLSW ltr dtd 2 May 1956; ASD ltr. dtd 17 Sept 1970

THIS PAGE IS UNCLASSIFIED

CLASSIFICATION CHANGED

CONFIDENTIAL

FROM CONFIDENTIAL TO UNCLASSIFIED
Insert Class Insert Class

173032

ON 8 May 1956 By authority of Reclass. List-77
Month Day Year Specify Authority Being Used

A. ASH...

This action was rendered by Arthur L. ...
Name in Full Date

REPRODUCTION QUALITY NOTICE

This document is the best quality available. The copy furnished to DTIC contained pages that may have the following quality problems:

- **Pages smaller or larger than normal.**
- **Pages with background color or light colored printing.**
- **Pages with small type or poor printing; and or**
- **Pages with continuous tone material or color photographs.**

Due to various output media available these conditions may or may not cause poor legibility in the microfiche or hardcopy output you receive.

If this block is checked, the copy furnished to DTIC contained pages with color printing, that when reproduced in Black and White, may change detail of the original copy.

SUBSONIC FLOW OVER A BODY BETWEEN POROUS WALLS

Rudolf R. Kasner
Aircraft Laboratory

February 1952

RDO No. R458-429

Wright Air Development Center
Air Research and Development Command
United States Air Force
Wright-Patterson Air Force Base, Ohio

Best Available Copy

ABSTRACT

The flow over a body at subsonic speeds in a tunnel equipped with porous walls is investigated. The problem is treated as two dimensional. The boundary condition assumed along the walls is that the pressure drop in the flow passing through the porous wall is a linear function of the cross flow velocity through the wall.

First, a general solution resulting in an image method is derived for the problem of an arbitrary two dimensional body in an infinite flow bounded by only one straight porous wall. Then, for two straight porous walls, an equally general method using repeated reflection is developed. The particular case of a thin circular cylinder (doublet disturbance) between two walls of equal porosity is solved in a closed mathematical form.

The distributions of pressure and velocity existing along the walls and along the centerline are discussed. Specifically, it is found that, in contrast to the case of solid walls, the flow around a symmetrical body between porous walls, e.g., a cylinder, is not symmetrical with respect to an axis perpendicular to the flow direction.

The security classification of the title of this report is CONFIDENTIAL.

PUBLICATION REVIEW

This report has been reviewed and is approved.

FOR THE COMMANDING GENERAL:

Robert R. Myers, Col

JACK A. MEERS, Colonel, USAF
Ch'ef, Aircraft Laboratory
Aeronautics Division

TABLE OF CONTENTS

| <u>Section</u> | <u>Page</u> |
|--|-------------|
| I The Flow Bounded by One Straight Porous Wall | 1 |
| The Composition of the Flow Field | 1 |
| The Boundary Condition | 2 |
| Description of the Solution | 3 |
| Velocities at the Wall | 4 |
| Application to the Flow Around a Small Cylinder | 5 |
| Conditions of Mass Flow Through a Wall | 8 |
| II The Problem of Two Straight Porous Walls | 9 |
| The Method of Iterated Reflection | 9 |
| Closed Mathematical Solution | 10 |
| Evaluation and Comparison of Results With Those Obtained for One Wall | 13 |
| III Representation of the Results by Dimensionless Parameters | 14 |
| IV Application of Results to Compressible Flow | 15 |
| V Summary | 16 |
| References | 17 |

[Handwritten marks]

CONFIDENTIAL

SECURITY INFORMATION

LIST OF ILLUSTRATIONS

| <u>Figure</u> | | <u>Page</u> |
|---------------|--|-------------|
| 1 | Flow Bounded by One Straight Porous Wall. | 18 |
| 2 | Velocity Diagrams of a Point P at the Wall for Different Porosities. | 18 |
| 3 | Doublet Flow and its Reflection at the Wall for Different Porosities. | 19 |
| 4 | Flow Bounded by Two Straight Porous Walls. | 20 |
| 5 | Doublet Patterns for Closed Walls and for Open Jet. | 20 |
| 6 | Doublet Pattern for One and Two Porous Walls ($\delta = 60^\circ$, $c = \sqrt{3}$). | 20 |
| 7 | Normal Velocity Component, V_y , Along Wall (One Wall). | 21 |
| 8 | Tangential Velocity Component, $V_{x_2} + V_{x_3} = V_x - V_\infty$, Along Wall (One Wall). | 22 |
| 9 | Ordinates $y - y_0$ of Boundary Streamline (One Wall) | 23 |
| 10 | Normal Velocity Component, $V_{y_2} + V_{y_3} = V_y$, Along Wall (Two Walls). | 24 |
| 11 | Tangential Velocity Component, $V_{x_2} + V_{x_3} = V_x - V_\infty$, Along Wall (Two Walls). | 25 |
| 12 | Ordinates $y - y_0$ of Boundary Streamline (Two Walls). | 26 |
| 13 | Wall Effect V_{x_3} Along Centerline $y = 0$ (Two Walls). | 27 |

CONFIDENTIAL

LIST OF SYMBOLS

| | |
|--------------|-----------------------------------|
| A | cross-sectional area of the body |
| C | coefficient of porosity |
| P | pressure |
| M_{∞} | Mach number at infinity |
| $f_c; f_s$ | functions of angle φ |
| i | imaginary unit |
| k | porosity constant of wall |
| n | number designating the doublets |
| P | $\frac{y_0^2}{x_0^2}$ |
| r_0 | radius of cylinder |
| V | velocity |
| x | ordinate parallel to the walls |
| y | ordinate normal to the walls |
| y_0 | distance of wall from nodal |
| $z = x + iy$ | complex variable |
| β | $\sqrt{1 - M_{\infty}^2}$ |
| σ | turning angle of image flow |
| λ_v | form coefficient |
| φ | angle of local vector with x axis |
| φ_0 | angle of doublet axis with x axis |
| ρ | density |

CONFIDENTIAL

LIST OF SYMBOLS (Continued)

ϕ flow potential
 ψ stream function

SUBSCRIPTS

1 denotes flowfield 1 (parallel flow)
2 denotes flowfield 2 (disturbances due to body)
3 denotes flowfield 3 (disturbances due to images)
 $3c$ denotes flowfield 3 of a closed wall
 ∞ infinitely far upstream or downstream
 x x-component
 y y-component

CONFIDENTIAL

INTRODUCTION

In the supersonic and in the transonic Mach number range, porous wind tunnel walls are known as means to approximate the conditions of a free airstream by partially eliminating the effects of closed tunnel walls. The object of the present report is to investigate the effect of porous walls on a subsonic flow.

The computations are carried through for incompressible flow. They are made applicable to compressible subsonic flow by means of the Prandtl-Glauert rule.

Part of the results obtained in this report are already contained in a report by Goodman (Reference 1). It came to the knowledge of the author at a time when the work on which this report is based was almost completed. The approach as presented in this report starts from the simple problem of the flow over a body in the neighborhood of one straight porous wall. Then, the solution for the main problem of a body between two porous walls will be derived from the results obtained for one wall. Furthermore, a rather extensive discussion of the results with an extension to compressible flow is given.

CONFIDENTIAL

SECTION I

THE FLOW BOUNDED BY ONE STRAIGHT POROUS WALL

The flow is treated as a potential flow from the fact that, through some parts of the wall, there is an inflow of air into the tunnel. The inflowing air has a lower total pressure than the main flow, because the total pressure outside the tunnel is lower than inside and because of pressure losses which the air undergoes when passing through the wall. Therefore, the flow inside the tunnel cannot rigorously be treated as a potential flow.

In the considered case where the cross-flow velocities are small, the inflowing air forms a thin layer adjacent to the inner side of the wall. In a rigorous first-order analysis, the effect of this layer of smaller total pressure must be taken into account.

In the present analysis, the simplifying assumption is made that potential flow prevails in the entire flow including the regions at the wall. It should be the subject of a further investigation to determine the influence due to the total pressure loss of the inflowing air.

The flow may be considered as superimposed from these three parts:

1. A flow field (1), representing a parallel flow with the velocity $V_1 = V_{x_1} = V_{\infty}$.
2. A flow field (2) with the velocity components V_{x_2}, V_{y_2} resulting from singularities inside or on the contour of the body.
3. A flow field (3) which is regular in the region inside the wall.

Flow field (3) can be described by singularities either on or outside the wall, e.g. by a distribution of sources or vortices along the wall. Consider the example of a closed (solid) wall. It is known that in this case flow field (3) is the image flow of field (2) with respect to the wall. If, for example, field (2) is represented by a doublet, field (3) is represented by a doublet in the image point.

Since flow field (2) is determined from the condition that the normal components resulting from the three flow fields vanish at the

CONFIDENTIAL

boundaries of the body, flow field (2) belonging to a certain body depends on fields (1) and (3).

However, in the considered case of a small body, the components of flow field (3) at the boundary of the body are small compared to V_{∞} ; therefore, flow field (2) can, in the first order analysis, be determined by the infinite airstream (1) alone. In the following, flow field (1) will be considered as known. Then flow field (3) will be found from the boundary condition at the porous wall which will be described by an equation connecting V_{y_3} and V_{x_3} along the wall with the velocities of flow fields (1) and (2).

It is noted that the distribution of either V_{y_3} or V_{x_3} along the wall is already sufficient to determine flow field (3). The distribution of V_{y_3} is equivalent to a source distribution and the distribution of V_{x_3} is equivalent to a vortex distribution along the wall.

Boundary Condition

The boundary condition is assumed to follow a linear relationship between the pressure P and the velocity, V_y , normal to the wall:

$$P - P_{\infty} = kV_y \quad (1)$$

where the left hand side is the pressure difference between points close to the tunnel wall inside and outside of the tunnel. The pressure outside of the tunnel is assumed to be equal to the pressure at infinity, P_{∞} . The pressure P for a point in the incompressible potential flow is computed from Bernoulli's equation

$$P - P_{\infty} = -\frac{\rho}{2} (V^2 - V_{\infty}^2)$$

Using linearization, i.e., neglecting terms with $(V_x - V_{\infty})^2$ and V_y^2 , one obtains

$$P - P_{\infty} = -\rho (V_x - V_{\infty}) \quad (2)$$

Equations (1) and (2) result in the boundary condition

$$V_x - V_{\infty} = -C V_y \quad (3)$$

or, applied to the particular case under consideration,

$$V_{x_2} + V_{x_3} = -C (V_{y_2} + V_{y_3}) \quad (4)$$

with

$$C = \frac{k}{\rho V_{\infty}} \quad (5)$$

as a parameter characterizing the porosity.

CONFIDENTIAL

Description of the Solution

The solution of Laplace's equation for the boundary conditions as given in the previous paragraph can be expressed for the general case of an arbitrary body in the presence of a straight porous wall in the following simple way.

If flow fields (1) and (2) are given, then in the case of a straight closed wall, flow field (3) can be found as the image of the flow field (2) with respect to the wall. This field may be denoted as field (3c).

The flow field (3) due to a porous wall of constant porosity can be obtained from the flow field (3c) by simply turning all velocity vectors of flow field (3c) by a given constant angle δ . This turning angle depends on the porosity according to

$$\cotan \frac{\delta}{2} = C. \quad (6)$$

In the case of Figure 1 (flow in the positive x direction, wall above the model), the velocity vector must be turned in the clockwise direction.

One has $\delta = 0$ for $C \rightarrow \infty$ (closed wall)

$\delta = 180^\circ$ for $C = 0$ (open boundary)

For finite porosities, the value of δ is between 0° and 180° as the following table shows:

| | | | | | | |
|--------------|------------|------------|------------|-------------|-------------|-------------|
| $C = \infty$ | 3.732 | 1.732 | 1 | .5773 | .2680 | 0 |
| $\delta = 0$ | 30° | 60° | 90° | 120° | 150° | 180° |

Verification of the Solution

It has to be proven that the general solution, as described in the previous paragraph, satisfies the Laplace differential equation as well as the boundary condition.

The solution can be expressed, using complex variables, by

$$(v_x + i v_y)_3 = e^{-i\delta} (v_x + i v_y)_{3c} \quad (7)$$

or, with the potential ϕ and the stream function ψ , by

$$(\phi + i\psi)_3 = e^{i\delta} (\phi + i\psi)_{3c} \quad (8)$$

That equations (8) and (7) are identical in that the velocity vectors of flow fields (8) are turned by δ relative to flow field (3c) can be seen

CONFIDENTIAL

by utilizing the relationship $\frac{d}{dz} (\phi + i\psi) = v_x - iv_y$ with $z = x + iy$.

The complex flow function $(\phi + i\psi)_{z_3}$ is a regular analytical function of z in the region $y < y_0$ because flow field (2) is regular in the region $y < y_0$ because field $3c$ is the image of field (2) with respect to the closed wall. Then, $(\phi + i\psi)_{z_3}$ is also a regular function of z because it results from multiplying $(\phi + i\psi)_{z_3c}$ with the complex constant $e^{i\delta}$. The differential equation is therefore satisfied.

In order to check the fulfillment of the boundary condition, eq. (7) is applied to the wall $y = y_0$. There $(v_x + iv_y)_{z_3c}$ can be replaced by $(v_x - iv_y)_2$. Furthermore, $e^{-i\delta}$ can be expressed by

$$e^{-i\delta} = \frac{e^{-i\frac{\pi}{2}}}{e^{i\frac{\pi}{2}}} = \frac{\cos\frac{\pi}{2} - i\sin\frac{\pi}{2}}{\cos\frac{\pi}{2} + i\sin\frac{\pi}{2}}, \text{ or, with eq. (6):}$$
$$e^{-i\delta} = \frac{C-i}{C+i} \quad (9)$$

therefore eq. (7) may be written

$$(v_x + iv_y)_3 (1 + C) + (v_x - iv_y)_2 (1 - C) = 0 \quad (10)$$

The imaginary part of eq. (10) is, in fact, identical with the boundary condition eq. (4).

Velocities at the Wall

The conditions along the wall are illustrated by Figure 2 which shows for different porosities, the velocity vectors V_2 and V_3 of a point at the wall. At the extreme left, for the closed wall, V_3 is marked by V_{3c} . Then follow from left to right cases of increasing porosities. V_3 is turned relative to the direction of V_{3c} by $(-\delta)$, i.e., in a clockwise sense.

Since V_3 and V_2 are vectors of equal length, the resultant vector $(V_2 + V_3)$ is turned by $(-\frac{\delta}{2})$ relative to the position parallel to the wall which it has for the closed wall.

The case $C = 0$ of the free boundary, represented in Figure 2 at the extreme right, is $\frac{\delta}{2} = 90^\circ$. This is in agreement with the condition of constant pressure and therefore constant velocity at the free boundary.

The velocity distribution along the wall itself is of particular interest because it illustrates to what degree the flow around a body in an infinite air stream can be approximated by an air stream bounded by porous walls.

CONFIDENTIAL

From eq. (7) for points at the wall

$$v_{x_3} = v_{x_2} \cos \delta - v_{y_2} \sin \delta \quad (11)$$

$$v_{y_3} = -v_{x_2} \sin \delta - v_{y_2} \cos \delta$$

Adding the components of flow fields (2) and (3) and expressing δ by C with

$$e^{-i\delta} = \cos \delta - i \sin \delta = \frac{C-1}{C+1} = \frac{C^2-1}{C^2+1} - i \frac{2C}{C^2+1} \quad (12)$$

one obtains

$$v_x - v_\infty = \frac{2C}{C^2+1} (v_{x_2} C - v_{y_2}) \quad (13)$$

$$v_y = -\frac{2}{C^2+1} (v_{x_2} C - v_{y_2})$$

The fulfillment of the boundary condition is evident from eqs. (13).

Furthermore, the flow over a body which is symmetrical in the x -direction, will generally, in the presence of a porous wall, have no properties of symmetry. This follows from the fact that for symmetrical bodies, v_{x_2} is symmetrical and v_{y_2} is antisymmetrical. According to

eq. (13), $v_x - v_\infty$ and v_y will then consist of symmetrical and antisymmetrical parts. The only exceptions are the cases $C = 0$ and $C = \infty$.

Application to the Flow Around a Small Cylinder

Let flow field (2), the disturbance due to the body, be a doublet at $x = 0, y = 0$; this represents the flow disturbance due to a circular cylinder of radius r_0 in a parallel flow with the velocity v_∞ in the x direction. Such a doublet flow is expressed by the following equations:

$$(\phi + i\psi)_2 = \frac{v_\infty r_0^2}{z} \quad (14)$$

or

$$\frac{d}{dz} (\phi + i\psi)_2 = v_{x_2} - i v_{y_2} = -\frac{v_\infty r_0^2}{z^2} \quad (15)$$

CONFIDENTIAL

After introducing an angle φ , defined by

$$\tan \varphi = \frac{z}{x} \quad (16)$$

the components along the wall according to eq. (15)

$$v_{x_2} = -v_{\infty} \frac{r_0^2}{y_0^2} \cdot f_0, \quad v_{y_2} = v_{\infty} \frac{r_0^2}{y_0^2} \cdot f_s \quad (17)$$

with

$$\begin{aligned} f_0 &= 1/2 (1 - \cos 2\varphi) - 1/4 (1 - \cos 4\varphi) \\ f_s &= 1/2 \sin 2\varphi - 1/4 \sin 4\varphi \end{aligned} \quad (18)$$

Inserting eq. (17) in eq. (13) yields the velocity components including the effect of the porous wall:

$$\begin{aligned} v_x - v_{\infty} &= -v_{\infty} \frac{r_0^2}{y_0^2} \frac{2C}{1+C^2} (Cf_0 + f_s) \\ v_y &= v_{\infty} \frac{r_0^2}{y_0^2} \frac{2}{1+C^2} (Cf_0 + f_s) \end{aligned} \quad (19)$$

These velocity distributions are plotted in Figures 7 and 8. The dimensionless scales used are explained in Sections III and IV. As marked before, the curves for finite porosities are unsymmetrical, v_x being symmetrical and v_y antisymmetrical.

For the closed wall ($C \rightarrow \infty$) a symmetrical pressure distribution exists as seen from the $(v_x - v_{\infty})$ distribution. When a small porosity (small openings) is introduced a small symmetrical v_y distribution results. This v_y -distribution is proportional to the pressure distribution. It yields an inflow through the part of the wall opposite the model while far upstream and downstream of the model small outflow velocities are produced. If the porosity is increased (decreasing C), v_y increases while $v_x - v_{\infty}$ (the pressure difference) decreases and both distributions, being always proportional to each other, become more and more unsymmetrical. Finally, for the open jet boundary, $C = 0$, v_y becomes antisymmetric and $v_x - v_{\infty}$ becomes zero.

The velocity distributions which would prevail along $y = y_0$ in an infinite flow over the cylinder are $v_x - v_{\infty} = v_{x_2}$ and $v_y = v_{y_2}$. They are marked in Figures 7 and 8 by dotted lines. These distributions are halfway between those for closed walls and those for the open jet boundary. v_x is symmetrical with respect to the X and Y axis and changes the sign

CONFIDENTIAL

at $\frac{x}{y} = \pm 1$. ($\frac{x}{y} = +1$ or $\varphi = 45^\circ$ and 135° are the directions where the streamlines of the doublet flow have vertical tangents.)

The flow field (3) resulting from a doublet in the presence of a porous wall has a particularly simple feature: It also represents a doublet flow.

This becomes obvious from eq. (3). The function $\phi + i\psi$ of a doublet flow field (3c) is

$$(\phi + i\psi)_{3c} = \frac{a}{z - b} \quad (20)$$

where a and b represent complex constants. After introducing polar coordinates r , from the center of the doublet, it assumes the form

$$(\phi + i\psi)_{3c} = \frac{a}{r e^{i\varphi}} = \frac{a}{r} e^{-i\varphi} \quad (21)$$

then, according to eq. (5), flow field (3) for a porous wall is

$$(\phi + i\psi)_3 = \frac{a}{r} e^{-i(\varphi - \sigma)}; \quad (22)$$

the result obviously is a doublet of the same strength and same location as doublet (3c). However, the main axis of the doublet (3), represented by the streamline $\psi = 0$, is turned by the angle σ with respect to the axis of doublet 3c.

The general result for the effect of a porous wall on a doublet flow therefore, can be expressed in the following manner:

The flow field (3) to be superimposed on the flow field (2) of the original doublet is equal to the image doublet existing in the case of a closed wall, but turned by the angle σ . σ is determined by the porosity according to $\sigma = 2 \cotan^{-1} C$. For later use, it shall be noted that the above statement is valid for any direction of the axis of doublet (3c) with respect to the porous wall.

Doublet (3) is turned with respect to doublet 3c in a counterclockwise sense, opposite to the sense in which the velocity vectors at individual points of the flow field are turned.

In the present case, doublet (2) is given by eq. (14) and doublet (3c) is orientated parallel to the wall. Then it follows for doublet (3) the center of which is in $z = 2i\sqrt{0}$

$$(\phi + i\psi)_3 = \frac{m \sqrt{0}^2}{z - 2i\sqrt{0}} e^{i\sigma}$$

CONFIDENTIAL

The disturbance flow field produced by the cylinder in presence of the porous wall is then

$$(\phi + i\psi)_{2+3} = v_{\infty} \frac{1}{\sigma} \left(\frac{1}{z} + \frac{e^{i\theta}}{z - 2iy_0} \right) \quad (23)$$

Doublet (3) is turned in such a way that an inflow through the part of the wall near the model is produced. This rule expresses the sense of turning independent of the location of the wall and of the flow direction.

Figure 3 shows schematically the position of the original and of the reflected doublet for different porosities and the distribution of $V_x - v_{\infty}$ and V_y which they produce along the wall.

Conditions of Mass Flow through the Wall

It can be seen from the general solution as well as in a particularly simple way, from the cylinder flow superimposed from two doublets, that the resulting flow through the entire length of the porous wall

$$\int_{-\infty}^{\infty} V_y dx \text{ is zero.}$$

In Figure 9, the displacements of the boundary streamline which coincide with the wall infinitely far upstream and downstream from the body is plotted in order to illustrate the mass flow through different parts of the wall. The mass flow through a part of the wall is given by the change of the stream function $\psi = \psi_{\text{wall}}$ along the wall. A small mass flow ($-d\psi_{\text{wall}}$) occurring through an element of the wall in the y -direction results in a displacement dy of the boundary streamline which according to the continuity equation, is

$$dy = -\frac{d\psi_{\text{wall}}}{V_x}.$$

The equation of the boundary streamline can be found from an integration when V_x is approximated by v_{∞} ,

$$y - y_0 = -\frac{\psi_{\text{wall}}}{v_{\infty}} \quad (24)$$

The stream function ψ_{wall} was obtained as the imaginary part of the function $\phi + i\psi$. Substituting in eq. (23) the angle φ defined by

$$\frac{y_0}{x} = \tan \varphi \quad (25)$$

yields

$$\psi_{\text{wall}} = \frac{v_{\infty} r_0^2}{\gamma_0} \sin \gamma \left[-\sin \varphi + \sin (\varphi + \delta) \right] \quad (26)$$

or, introducing the porosity constant C instead of δ according to eq. (6),

$$\psi_{\text{wall}} = \frac{v_{\infty} r_0^2}{\gamma_0} \frac{1}{1 + C^2} \left[(1 - \cos \bar{\varphi}) - C \sin \gamma \right] = -(y - y_0) v_{\infty} \quad (27)$$

SECTION II

THE PROBLEM OF TWO STRAIGHT POROUS WALLS

The two-dimensional flow in a tunnel bounded by two parallel straight porous walls will now be investigated.

The Method of Iterated Reflection

The solution for two walls can be derived from the solution found for one wall. First, the change of the flow field due to one wall is determined. Then, the second wall is taken into account, since, due to the second wall, the conditions at the first wall are changed. The effect of the first wall will also change, etc. Thus, a method of iterated reflection results which applies to any shape of the body.

As an example, the above method will now be applied to the case (Figure 4) where both walls located at $y = y_0$ and $y = -y_0$ are of equal porosity and where the body (model) is again represented by a doublet disturbance.

It is known that for the case of two closed walls, and for the case of two free boundaries (open jet), this method leads to an infinite set of doublets located along the y -axis at $y = 2ny_0$ with $n = 0, \pm 1, \pm 2, \text{ etc.}$ For the closed tunnel walls, the main axes of all doublets are parallel to the walls and have the same direction; for the open jet, consecutive doublets have opposite directions (Figure 5).

It will be shown that in the case of two porous walls, a pattern of doublets located at the same points $x = 0, y = 2ny_0$ results. Starting from the original doublet, D_0 located in $x = 0, y = 0$, the influence of wall one at $y = y_0$ consists of the image doublet D_1 at $x = 0, y = 2y_0$ (Figure 6). The influence of wall two in $y = -y_0$ then consists of the images of D_0 and D_1 with respect to wall two; i.e., D_{-1} located at $y = -2y_0$ and D_{-2} located at $y = -4y_0$. The effect of the first wall now has to be corrected in as far as the images of D_{-1} and D_{-2} with respect to wall one have to be added. They are D_2 located at $y = 4y_0$ and D_3 located at

CONFIDENTIAL

By repeating the above procedure, an infinite set of doublets located at the points $z = n2iy_0$ arises. The equation of each of these doublet flow fields is easily found from eq. (8).

The result is that the main axes of the doublets $D_1, D_2,$ and D_3 are turned by the angles $\delta, 2\delta, \dots, n\delta$, relative to the x-axis, while the main axes of $D_{-1}, D_{-2},$ etc. are turned by the angles $(-\delta), (-2\delta),$ etc. (Figure 6).

The resulting flow function, including the original doublet at $x = 0, y = 0$ is

$$(\phi + i\psi)_{2+3} = v_{\infty} \frac{2}{y_0} \cdot \sum_{n=-\infty}^{\infty} \frac{e^{in\delta}}{z - n2iy} \quad (28)$$

Closed Mathematical Solution

It is possible to obtain a closed mathematical expression instead of the infinite series eq. (28) derived in the previous paragraph.

For the case $\delta = 0$ (closed walls) the solution is known to be (see e.g. Reference 2):

$$(\phi + i\psi)_{2+3} = v_{\infty} \frac{2}{y_0} \frac{\pi}{2y_n} \cdot \coth\left(\frac{\pi}{2y_0} z\right) \quad (29)$$

The fact that eq. (29) is identical with eq. (28), if $\delta = 0$, can be derived from the relationship $\coth(iu) = -i \cotan u$ and from the series (see e.g. Reference 3)

$$\cotan u = \frac{1}{u} + \frac{1}{u-\pi} + \frac{1}{u+\pi} + \frac{1}{u-2\pi} + \frac{1}{u+2\pi} + \dots + \frac{1}{u-n\pi} + \dots \quad (30)$$

The proof of eq. (30) may, for any complex variable u , according to a theorem by Cauchy (Reference 4), be based on the property that the series on the right-hand side coincides with the function on the left-hand side with respect to the singularities and to their behavior at infinity. In the vicinity of each of the singular points $u = n\pi$, the function $\cotan u$ is indeed asymptotically represented by the term

$$\frac{1}{u - n\pi} \text{ of the series eq. (30).}$$

In the same way, it will now be attempted, for the case of porous walls, to find a closed expression which coincides with the series expression eq. (28) at the singular points and at infinity.

The singularities which the expression eq. (28) has at the points $z = n2iy_0$, are obtained from the denominators, which eq. (28) has in the

CONFIDENTIAL

case $\delta = 0$, if each singularity is multiplied by $e^{i\delta z}$. Therefore the desired closed expression replacing eq. (28) will result if the closed expression for $\delta = 0$, eq. (29), is multiplied by an integral function which is equal to $e^{i\delta z}$ at the points $z = 2niy_0$. This multiplying function is readily found to be $e^{\frac{z}{2y_0} \delta}$. The closed form of the solution for porous walls is therefore

$$(\phi + i\psi)_{2+3} = v_{\infty}^2 r_0^2 \frac{\pi}{2y_0} [\coth\left(\frac{\pi}{2y_0} z\right) - a] e^{\frac{\delta}{2y_0} z} \quad (31)$$

The constant $(-a)$ has been added in order to fulfill the condition that $\phi + i\psi$ is finite at $z \rightarrow \infty$, where $\coth\left(\frac{\pi}{2y_0} z\right)$ becomes 1. While this condition is satisfied by $a = 0$ for the case $\delta = 0$ (closed walls), it requires for $\delta \neq 0$ (porous walls) the value $a = 1$.

With $a = 1$ the solution may also be written

$$(\phi + i\psi)_{2+3} = v_{\infty}^2 r_0^2 \frac{\pi}{y_0} \frac{e^{\frac{\delta}{2y_0} z}}{e^{\frac{\pi}{y_0} z} - 1} \quad (32)$$

In order to obtain velocity components, eq. (32) is differentiated:

$$\frac{d}{dz} (\phi + i\psi)_{2+3} = (v_x - i v_y)_{2+3} = -\pi v_{\infty}^2 r_0^2 \frac{e^{\frac{\delta}{2y_0} z}}{[e^{\frac{\pi}{y_0} z} - 1]^2} + (\pi - \frac{\delta}{2}) e^{\frac{\delta}{2y_0} z} \frac{e^{\frac{\pi}{y_0} z}}{[e^{\frac{\pi}{y_0} z} - 1]^2} \quad (33)$$

Along the upper wall $y = y_0$, the velocity components are:

$$v_{x_{2+3}} = v_x - v_{\infty} = -q \cos \frac{\delta}{2} \quad \text{with } q = \pi v_{\infty}^2 r_0^2 \frac{e^{\frac{\delta}{2y_0} x}}{[e^{\frac{\pi}{y_0} x} - 1]^2} + (\pi - \frac{\delta}{2}) e^{\frac{\delta}{2y_0} x} \frac{e^{\frac{\pi}{y_0} x}}{[e^{\frac{\pi}{y_0} x} - 1]^2} \quad (34)$$

$$v_{y_{2+3}} = v_y = q \sin \frac{\delta}{2}$$

The stream function along the wall is

$$\psi_{\text{wall}} = -v_{\infty}^2 r_0^2 \frac{e^{\frac{\delta}{2y_0} x}}{[e^{\frac{\pi}{y_0} x} - 1]^2} \sin \frac{\delta}{2} \quad (35)$$

BOUNDARY LAYER

As in Section II for one wall, the ordinates y of the boundary streamlines which coincide with the wall $y = y_0$ at $x \rightarrow \infty$ are computed from

$$y - y_0 = - \frac{\psi_{\text{wall}}}{V_{\infty}} \quad (36)$$

These are plotted in Figure 12.

Finally, the velocity along the centerline was obtained by inserting $y = 0$ into eq. (33)

$$V_{2+3} = V_x - V_{\infty} = -\pi V_{\infty} \frac{r_0^2}{y_0^2} \frac{\frac{d}{2} \frac{x}{y_0} + (\pi - \frac{d}{2})^2 (\pi + \frac{d}{2}) \frac{x}{y_0}}{\left[\frac{d}{2} \frac{x}{y_0} - 1 \right]^2} \quad (37)$$

The velocity V_3 as plotted in Figure 13 represents the wall effect alone; it was obtained by subtracting from eq. (37) the velocity

$$V_2 = - \frac{r_0^2}{x^2} \quad (38)$$

which is produced along the centerline by the original doublet. However, for the point $x = 0$, the expressions eq. (37) and eq. (38) are infinite; therefore V_3 must be determined by a limiting process. The result at $x = 0$ is

$$V_3 = V_{\infty} \frac{r_0^2}{y_0^2} \frac{\pi^2}{2} \left[\frac{1}{6} - \left(\frac{d}{2r}\right) + \left(\frac{d}{2r}\right)^2 \right] \quad (39)$$

One may ask whether the porosity can be chosen in such a way that V_3 at the location $x = 0$, $y = 0$ of the model vanishes. This is actually the case for

$$\frac{d}{2} = \frac{\pi}{2} \left(1 - \frac{1}{\sqrt{3}} \right) = 35.04^\circ \quad (40)$$

or

$$C = \cotan \frac{d}{2} = 1.2500$$

The closed expression eq. (32) for $\phi + i\psi$ which was derived here from the series expression eq. (29), as well as the numerical result of eq. (40) are in agreement with the formula which R. Goodman (Reference 1) derived by means of a Fourier integral.

CONFIDENTIAL

Evaluation and Comparison of Results With Those Obtained for One Wall

As in case of one wall, the components along the wall and the mass flow through the wall are plotted (Figures 10 - 12) together with the flow conditions of the infinite airstream.

The velocity distributions resemble those obtained for the case of one wall.

A difference, however, exists in the case of two walls in as far as the resulting inflow through the parts of the porous walls close to the cylindrical body is compensated by an outflow through only the upstream parts of the walls (not upstream and downstream as in case of one wall).

For $C \rightarrow \infty$, i.e. closed walls, $V_x = V_{\infty}$ (the pressure) does not change the sign anywhere along the walls. This follows from the continuity condition: Since everywhere along the centerline between the walls V_x is less than V_{∞} due to the model influence, V_x is larger than V_{∞} everywhere along the walls.

A further deviation which will be noticed is a stronger rate of decrease for $x \rightarrow \pm\infty$, according to the exponential function. For this reason, the displacement of the boundary streamline represented by Figure 12, is smaller than for one wall (Figure 9). It is remarkable that the decrease downstream is greater than upstream.

The velocity $V_3 = V_{x3}$ along the centerline is plotted in Figure 13.

The curves $C \rightarrow \infty$ and $C = 0$ are both symmetrical. At the point $x = 0$, where the model is located, the influence V_3 of the open jet is one-half of the influence of closed walls and of opposite sign.

Furthermore, a comparison with Figure 11 shows that the velocity caused by closed walls at the location of the body ($x = 0$ on the centerline) is equal to one-third the sum $V_2 + V_3 = V_x = V_{\infty}$ which is produced at the wall.

The curves for the velocity distribution along the centerline (Figure 13) are unsymmetrical for all porosities different from zero and infinity. At $x = 0$, the location of the model, a finite V_3 as well as a

finite $\frac{dV_3}{dx}$ exists, i.e. a pressure disturbance as well as a pressure gradient exists. The only exception is the curve $C = 1.28$ with $V_3 = 0$ at $x = 0$. The curve $C = 1.28$ therefore characterizes the porosity for which the pressure disturbance due to the walls at the location of the model vanishes.

Nevertheless this case is not satisfactory, in as far as a pressure gradient exists at the model, and the wall interference is not eliminated.

REPRESENTATION OF THE RESULTS BY DIMENSIONLESS PARAMETERS

The graphs, Figures 7 - 15, represent the results in a dimensionless form. Eqs. (19) and (34), for the velocity components, can be written in such a way that the dimensionless magnitudes $\frac{v_x - v_\infty}{v_\infty} \cdot \frac{y_0^2}{r_0^2}$ and $\frac{v_y}{v_\infty} \cdot \frac{y_0^2}{r_0^2}$ appear as functions of $\frac{x}{y_0}$. From eq. (27), and from eqs. (35) and (36)

for the boundary streamline, the dimensionless ratio $\frac{r - r_0}{r_0} \cdot \frac{y_0^2}{r_0^2}$ can be derived which is also a function of $\frac{x}{y_0}$. The above dimensionless parameters were used as coordinates in the graphs.

Furthermore, it should be noted that the application of the results is not restricted to circular cylinders. The flow disturbance of cylindrical bodies of arbitrary cross section (without lift) is at some distance from the body essentially represented by a doublet flow. The strength of the doublet is (see Reference 5 and 6)

$$\frac{\lambda_v}{2} \Lambda \times v_\infty$$

where Λ is the cross-sectional area. λ_v is a factor which depends on the form of the cross section. For elliptical cross sections with the thickness ratio $\frac{b}{c}$,

$$\lambda_v = 1 + \frac{b}{c}$$

which yields $\lambda_v = 1$ for very slender elliptical shapes and $\lambda_v = 2$ for circular cross sections.

Therefore, in order to make the results applicable to arbitrary cylindrical bodies, the term $\pi r_0^2 v_\infty$ for the doublet strength has to be replaced by $\frac{1}{2} \lambda_v \Lambda v_\infty$. Thus, the dimensionless ordinates appearing on the graphs are $\frac{v_x - v_\infty}{v_\infty} p$; $\frac{v_y}{v_\infty} p$ and $\frac{r - r_0}{r_0} p$ where $p = \frac{y_0^2}{r_0^2}$ for circular cylinders and $p = \frac{y_0^2}{\lambda_v} \frac{\Lambda}{r_0^2}$ for arbitrary cylindrical bodies.

SECTION IV

APPLICATION OF RESULTS TO COMPRESSIBLE FLOW

In order to make use of the results for compressible subsonic flow, the Prandtl-Glauert rule may be applied. This application is restricted to slender bodies by the condition that the disturbance velocities are small, compared to V_{∞} , in the entire flow field.

According to the version of applying the Prandtl-Glauert rule, suggested by Goethert (Reference 6), the relationships found for incompressible flow remain valid for compressible flow if the magnitudes x , y , V_{∞} , $V_x - V_{\infty}$, V_y of the incompressible flow are replaced by the magnitudes x , βy , V_{∞} , $\beta^2(V_x - V_{\infty})$, βV_y with $\beta = \sqrt{1 - M_{\infty}^2}$ where M_{∞} is the Mach number of the compressible flow at infinity. Consequently, the cross-sectional area A appearing in the relationships for the incompressible flow around slender bodies has to be replaced by βA in the case of compressible flow.

With respect to the dimensionless coordinates of the graphs, as explained in Section III, it follows that they have to be replaced by

$$\frac{V_x - V_{\infty}}{V_{\infty}} \rho \beta^3; \frac{V_x}{V_{\infty}} \rho \beta^2; \frac{y - y_0}{y_0} \rho \beta; \text{ and } \frac{x}{x_0} \frac{1}{\beta}.$$

With respect to the parameters of the curves, it follows from the definition $C = \frac{V_x - V_{\infty}}{V_y}$, that it has to be replaced by $-\frac{V_x - V_{\infty}}{V_y} \beta = C\beta$.

This means that the parameter of the curves to be used in the case of compressible flow is $\beta = \sqrt{1 - M_{\infty}^2}$ times the actual porosity constant C of the wall. If the Mach number increases towards one, the parameter βC of the curve to be read approaches zero. Therefore, when the Mach number approaches one, a wall with any porosity different from zero produces a flow which approaches the characteristics of a free jet.

However, it should be noted that the above result is valid only in the case that the relationship between the cross flow velocity through a porous wall and the pressure drop is linear, and independent from the Mach number of the main flow, i.e., only as long as $P - P_{\infty} = k V_y$.

If there is a quadratic relationship, e.g. $P - P_{\infty} = k V_y^2$, the parameter of the curves in Figures 7 - 13 will not change with Mach number. Therefore, such a tunnel with a wall of finite porosity will maintain the characteristics of a partially open tunnel and will not approach the characteristics of an open jet when the Mach number in the tunnel approaches one.

SECTION 7

SUMMARY

With the assumptions that a linear relationship exists between the velocity components at the porous walls and that the flow including the region at the wall is a potential flow, the following results for infinitely long walls are obtained:

1. The wall interference can be eliminated by a suitable choice of the porosity constant only to the extent that the velocity disturbance due to the wall is made zero at one point of the flow field, e.g., at the center of the model. A pressure gradient will then still exist at the model.
2. The velocities in a flow field between porous walls are essentially different from the velocities of an infinite airstream around the same body. For a body which is symmetrical with respect to a plane perpendicular to the flow direction, the flow between porous walls is no longer symmetrical.
3. There is an inflow through the parts of the porous walls close to the body and an outflow through the other parts. The resulting flow through the entire wall is zero.
4. The outflow occurs through the upstream parts of the walls in the case of a circular cylinder between two porous walls. In the case of a cylinder in the vicinity of one porous wall bounding an infinite airstream, the outflow occurs upstream as well as far downstream of the body. Except for this difference the velocity distributions for the cases of one wall and of two walls agree rather closely.
5. Within the validity of the Prandtl-Glauert rule, it was found that the characteristics of a compressible flow around a slender model between walls of finite porosity approach the characteristics of a free jet when the Mach number approaches one. This is valid as long as the relationship between cross flow velocity through the porous wall and the pressure drop is linear and independent from the Mach number of the main flow.

REFERENCES

1. Cochran, Theodore B. The Porous Wind Tunnel, Part II. Cornell Aeronautical Laboratory Internal Research Project Report Number ATR-43, November 1950, p. 9. (Confidential, English)
2. Mueller, Wilhelm. Mathematische Stromungslehre. Berlin, Springer 1928, p. 83. (Unclassified, German)
3. Knopp, Konrad. Theory of Functions, Part II. Dover Publications, 1947, p. 44.
4. Copson, E. T. An Introduction to the Theory of Functions of a Complex Variable. Oxford University Press, pp. 146 - 148.
5. Glauert. Research and Memorandum 1566, p. 53.
6. Cothert, B. Windkanalkorrekturen bei hohen Unterschallgeschwindigkeiten. Jahrbuch der Deutschen Luftfahrtforschung 1941, Seite 1684. (Unclassified, German)

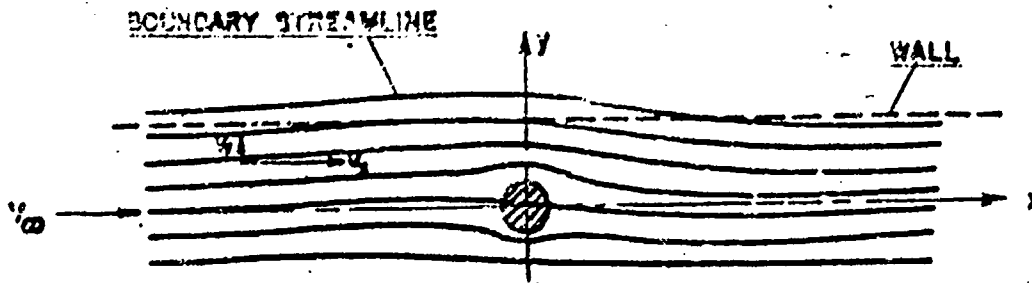


Figure 1: Flow Bounded by One Straight Porous Wall.

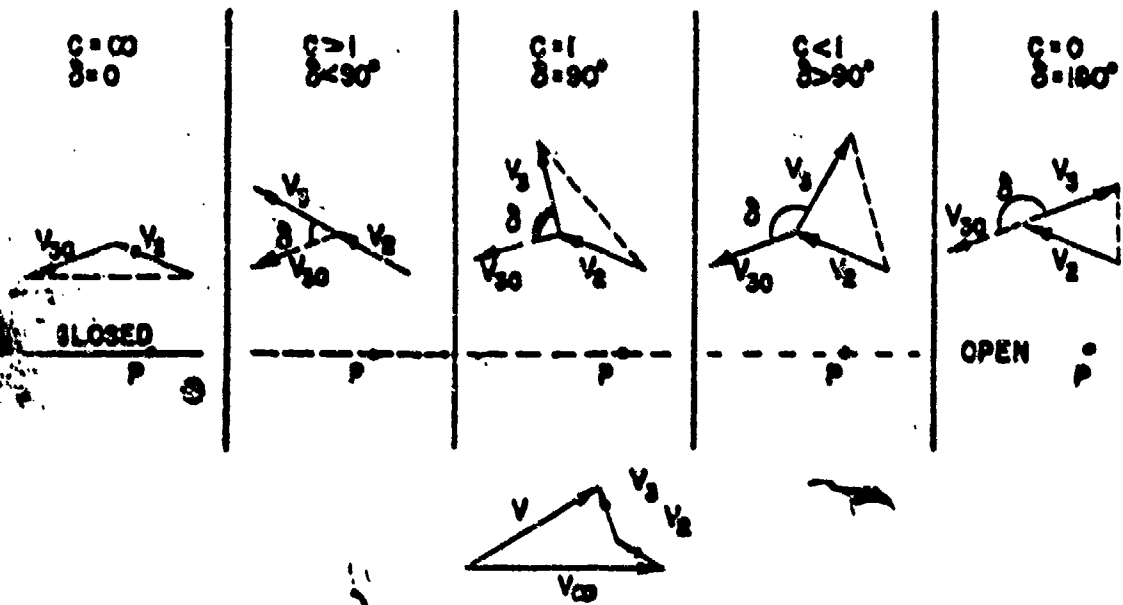


Figure 2: Velocity Diagrams of a Point P at the Wall for Different Porosities.

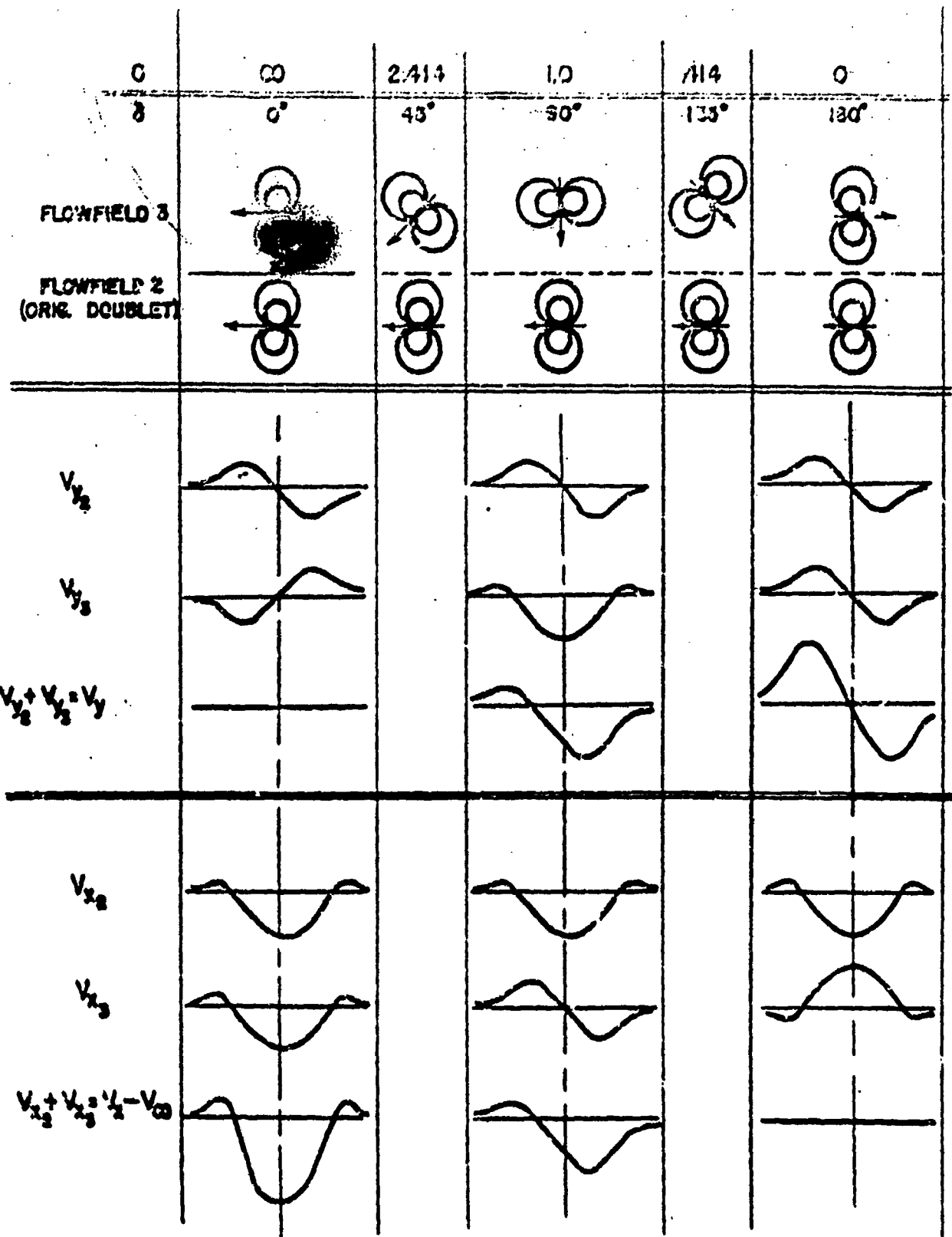


Figure 3: Doublet Flow and its Reflection at the Wall for Different Positions.

ADC-53-9

BOUNDARY STREAMLINE

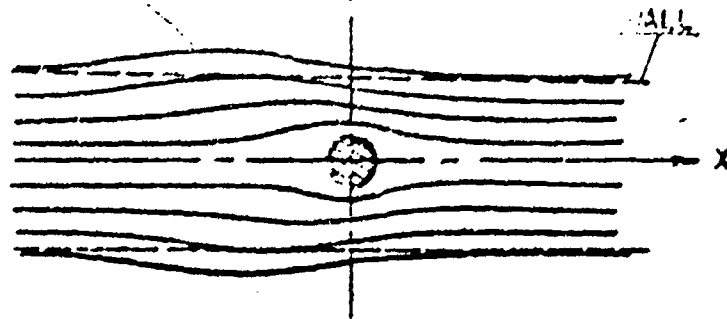


Figure 4: Flow Bounded by Two Straight Porous Walls.

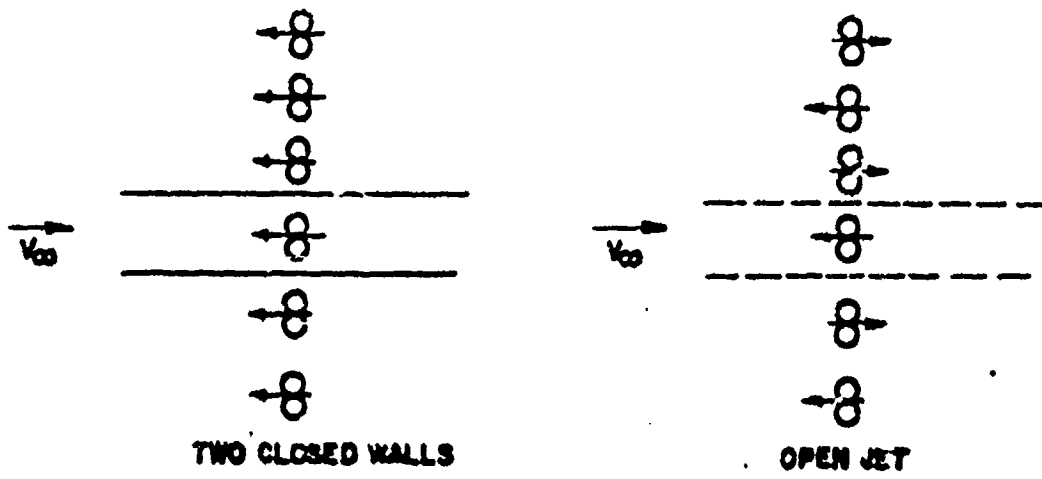


Figure 5: Doublet Patterns for Closed walls and for Open Jet.

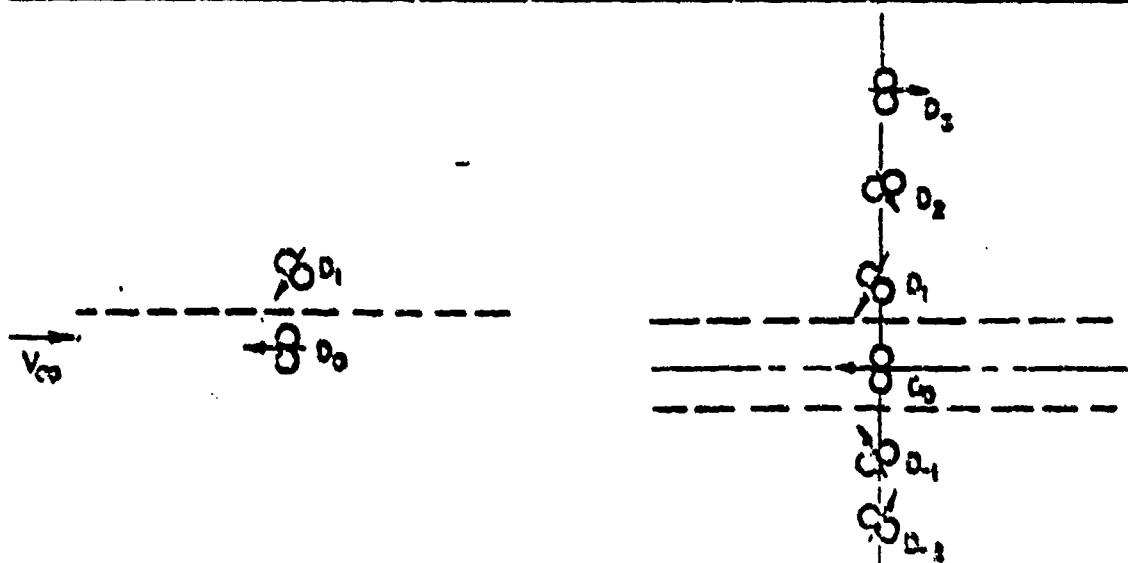
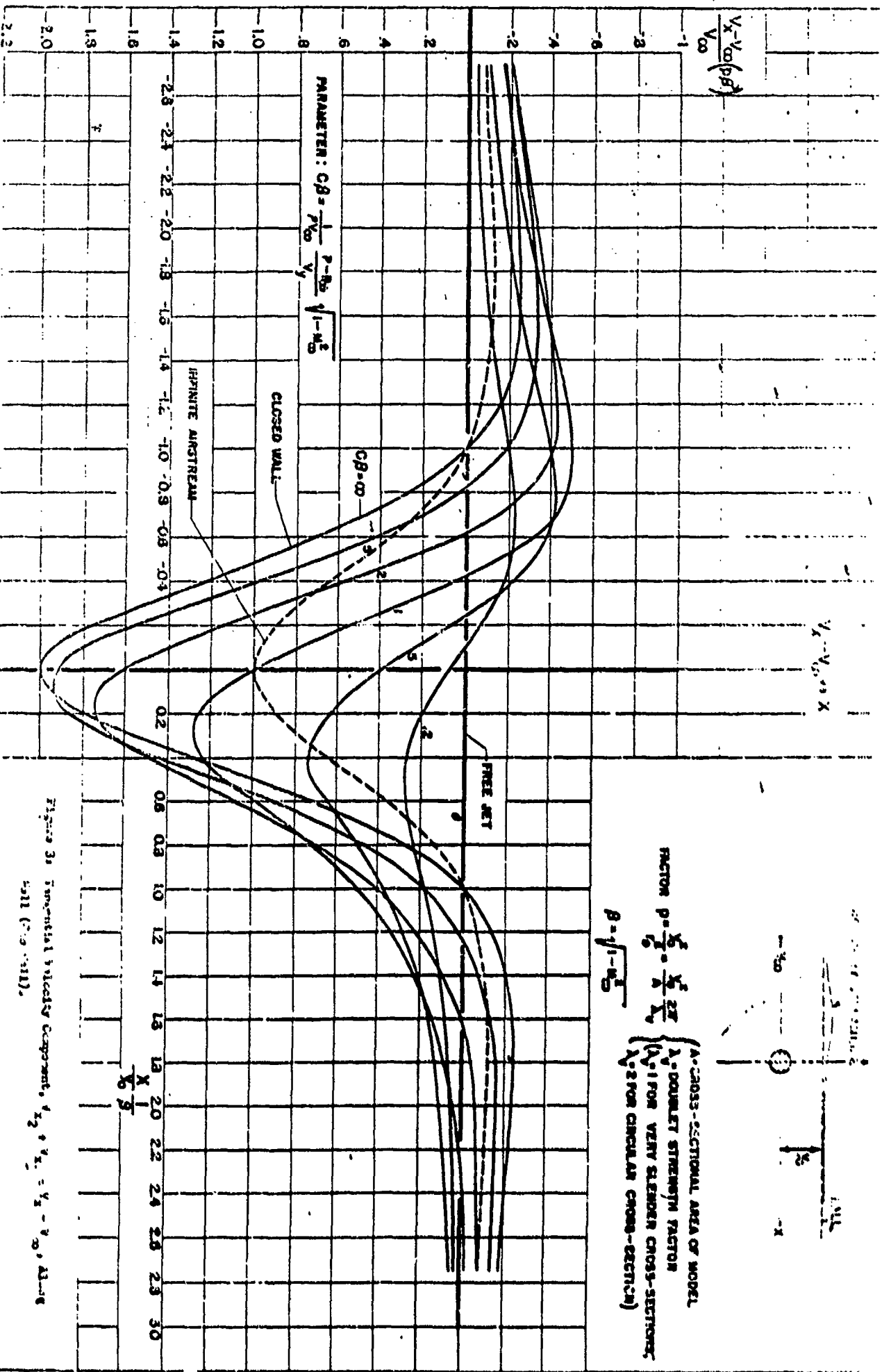


Figure 6: Doublet Pattern for One and Two Porous Walls ($\sigma = 60^\circ$, $C = \sqrt{3}$).

REC-52-9

CONFIDENTIAL



FACTOR $p = \frac{X}{S} \cdot \frac{X}{S} \cdot \frac{X}{S} \cdot 2\pi$

$\beta = \sqrt{1 - M_\infty^2}$

(A) DOUBLE-SECTIONAL AREA OF MODEL
 (B) DOUBLE STREAM FLOW
 (C) FOR VERY SLIM CROSS-SECTION
 (D) FOR CIRCULAR CROSS-SECTION

Figure 3: Potential Velocity Component, $V_x + V_x' = V_x - V_\infty$, Along Wall (See VIII).

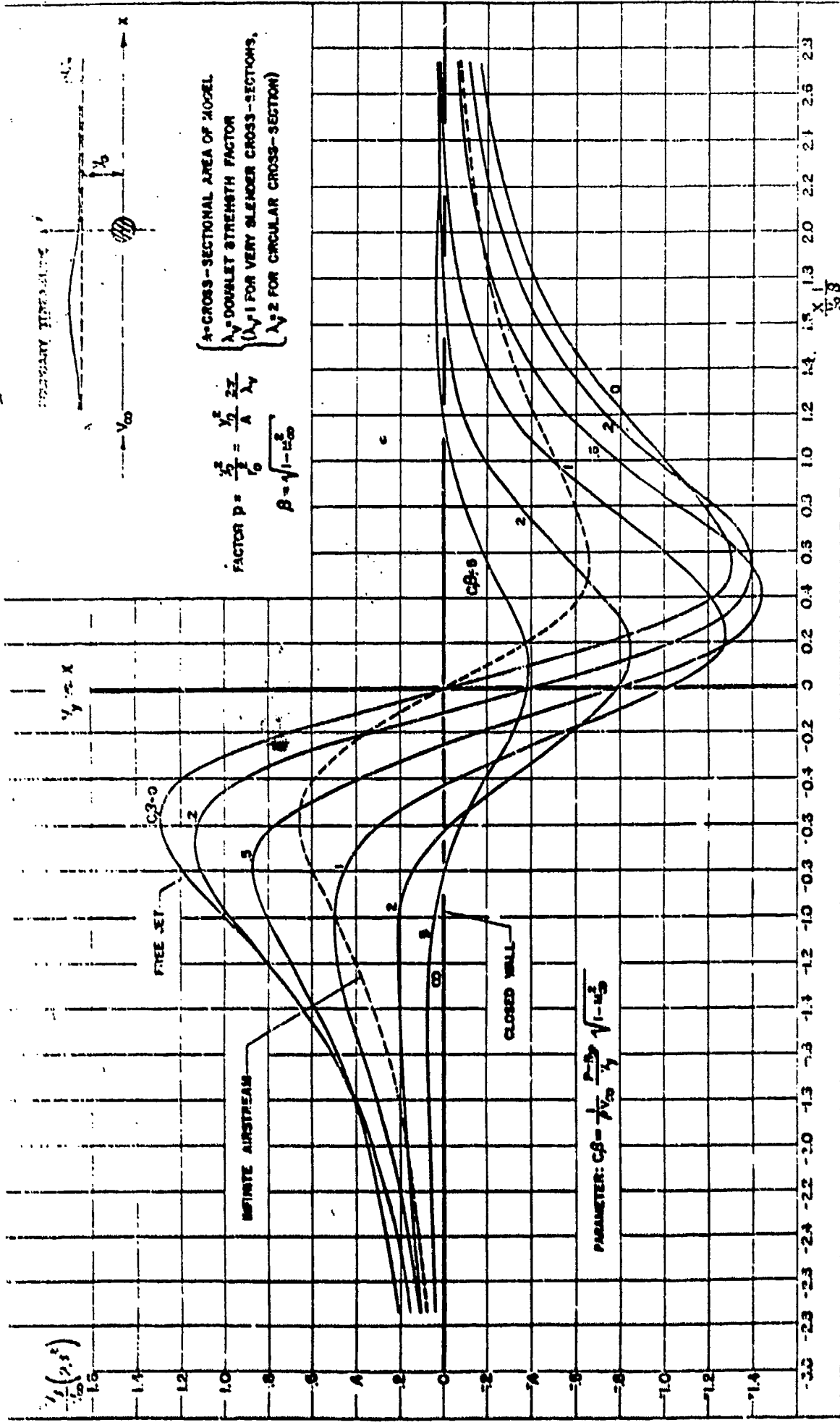


Fig. 7: Normal Velocity Component, v_y , Along Wall (One Wall).

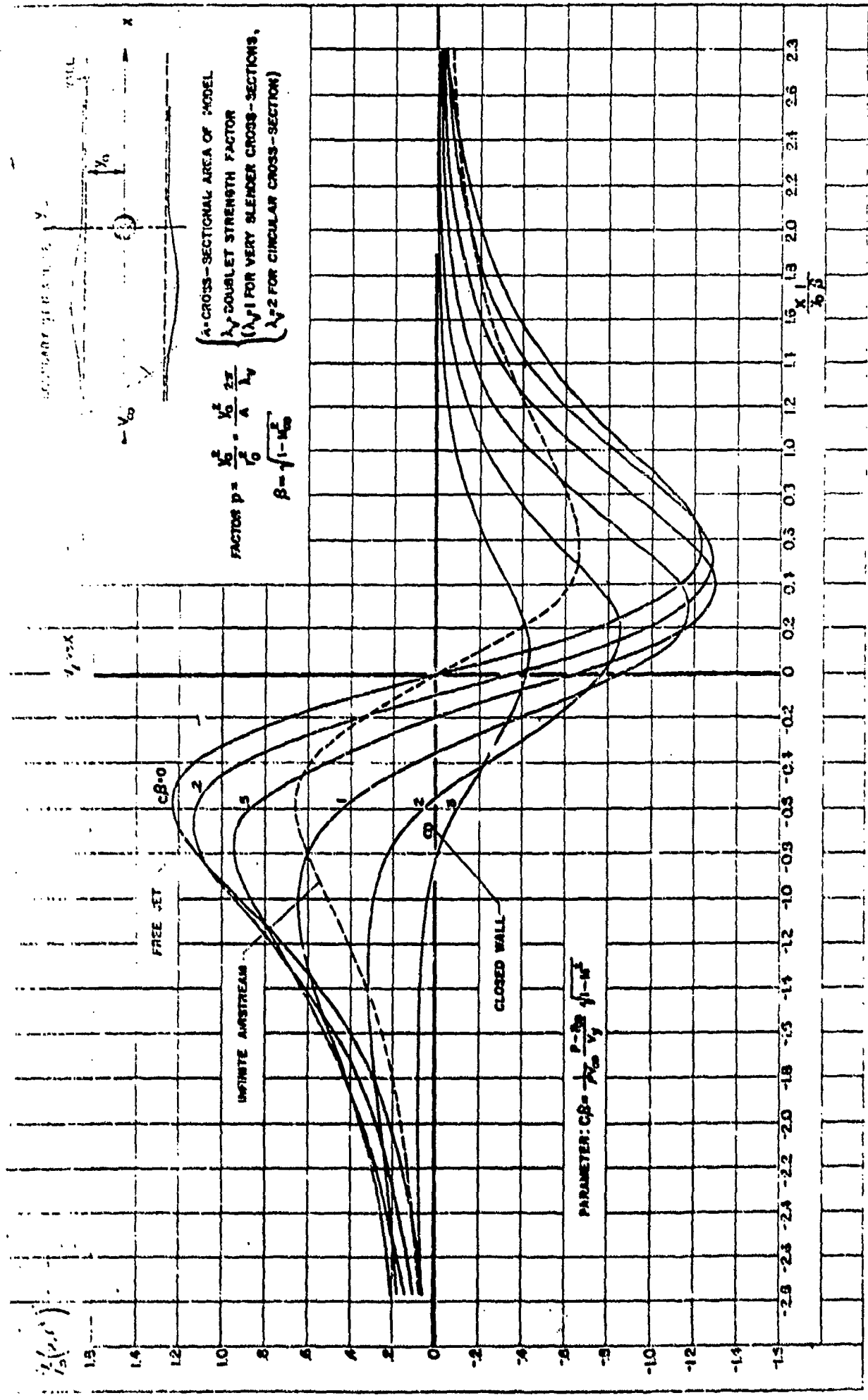


Figure 10: Lateral Velocity Component, $v_2 + v_1 = v$, Along shell (r = 0.011).

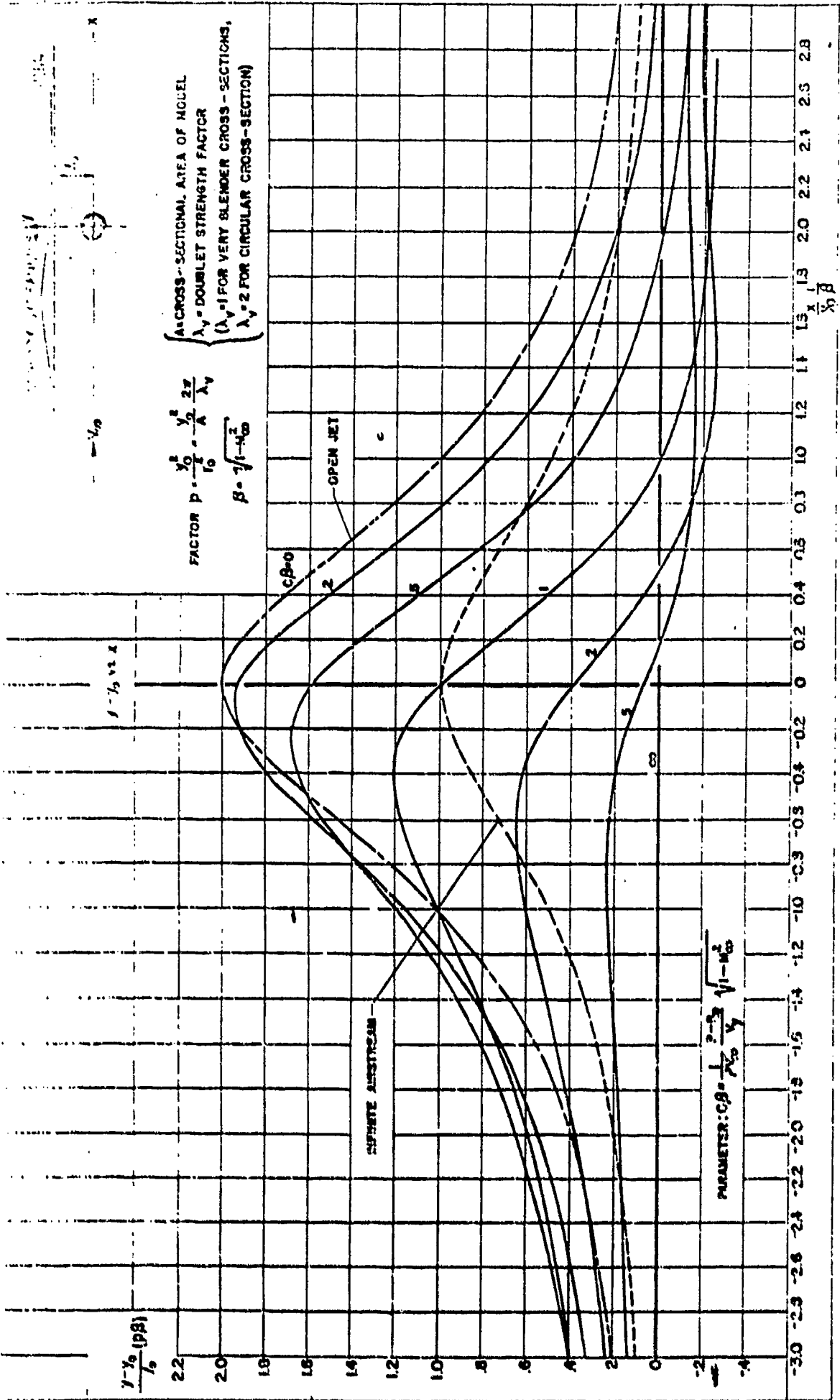
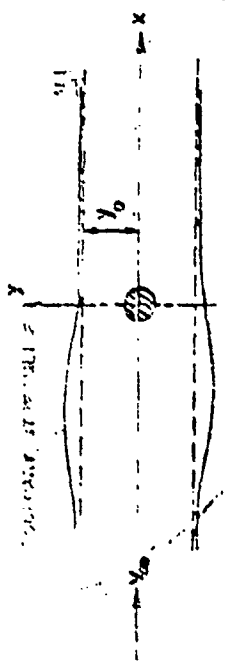


Figure 9: Coordinates $y - y_0$ of secondary streamlines (One - all).



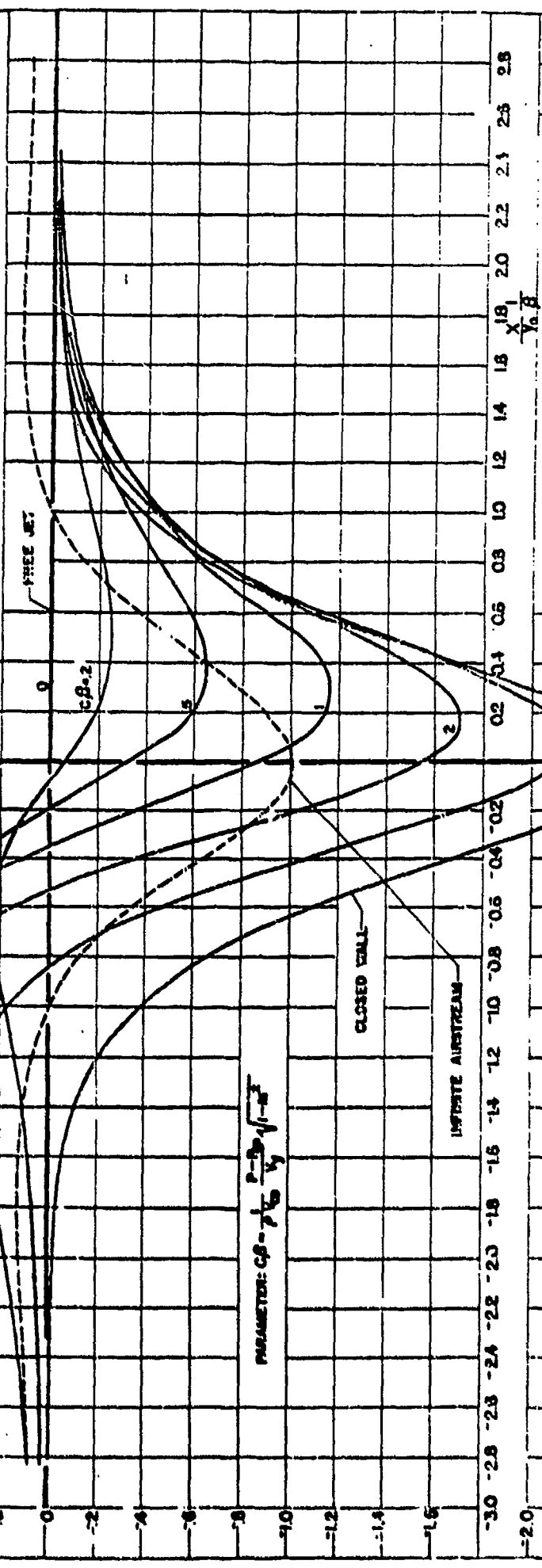
λ - CROSS-SECTIONAL AREA OF MODEL
 λ_0 - DOUBLET STRENGTH FACTOR
 $(\lambda_0 \neq 1 \text{ FOR VERY SLENDER CROSS-SECTIONS, } \lambda_0 = 1 \text{ FOR CIRCULAR CROSS-SECTION})$

$$\text{FACTOR } \rho = \frac{V_0^2}{6} = \frac{V_0^2}{6} \frac{2\lambda}{\lambda_0}$$

$$\beta = \sqrt{1 - u_0^2}$$

$$V_x = V_0 \sqrt{1 - \beta^2}$$

$$\frac{V_x^2}{V_0^2} = 1 - \beta^2$$



$$\text{PARAMETER: } c\beta = \frac{P - \rho V_0^2}{\rho V_0^2} \sqrt{1 - \beta^2}$$

Figure 11: Tangential Velocity Component,
 $V_{\theta_2} = V_0 \sqrt{1 - \beta^2} \frac{x}{\beta}$, Along Wall (See Wall)

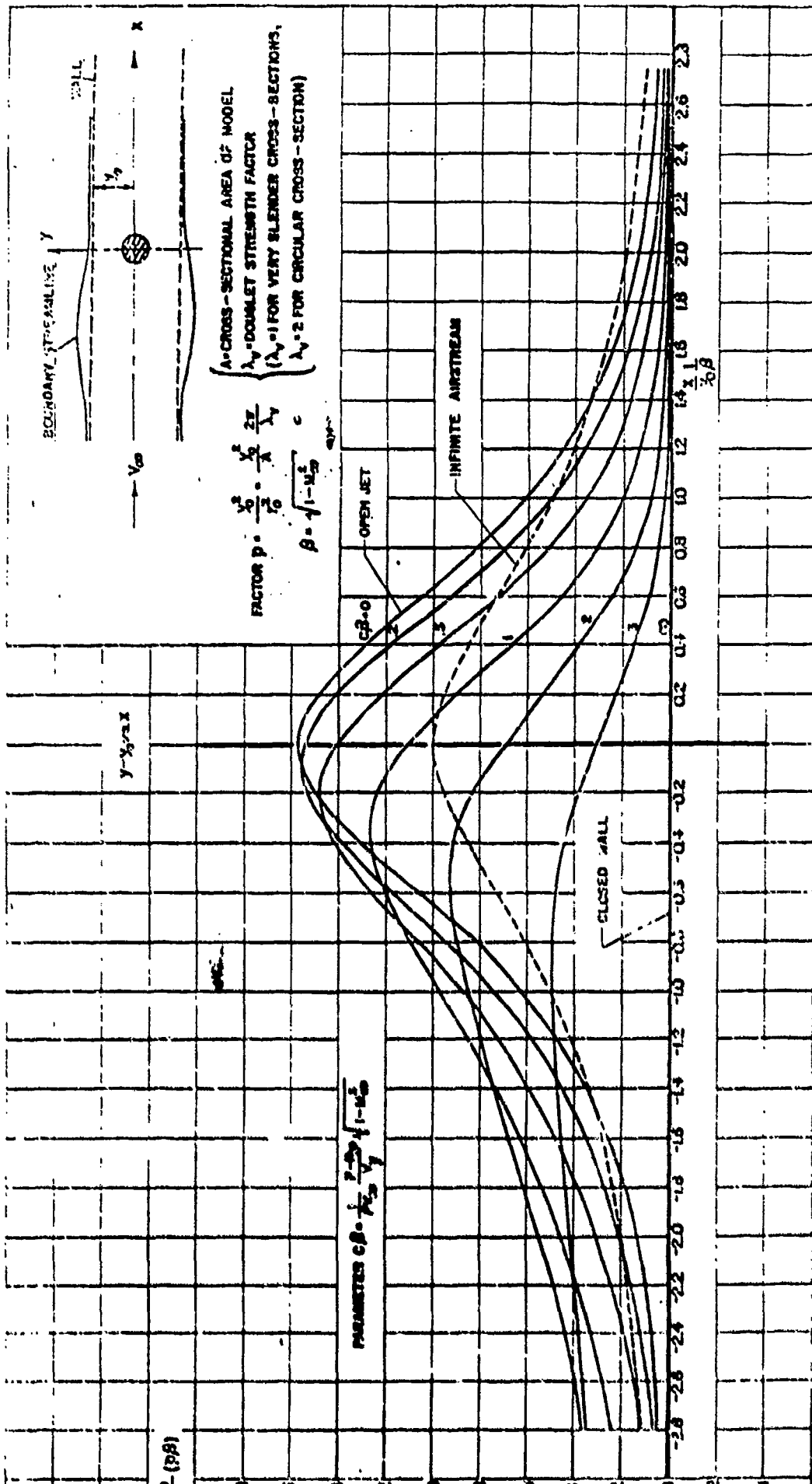
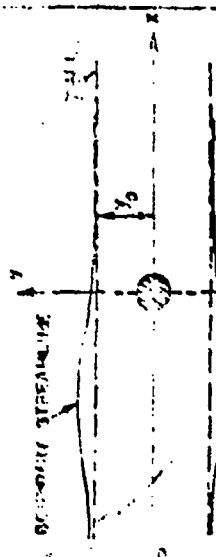


Figure 101 Coordinates $y - y_0$ of Boundary Streamlines (Two Cells).

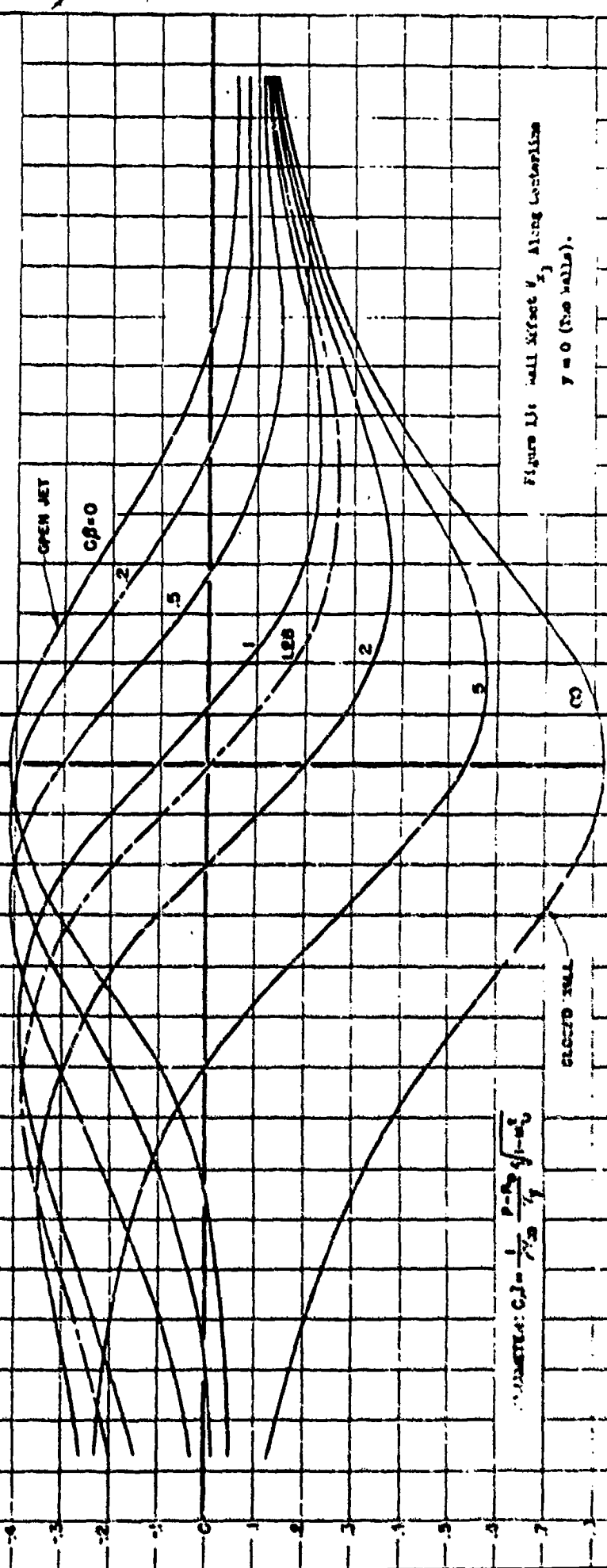


A-CROSS-SECTIONAL AREA OF MODEL
 A_0 -DOUBLET STRENGTH FACTOR
 $\lambda_0=1$ FOR VERY SLENDER CROSS-SECTIONS,
 $\lambda_0=2$ FOR CIRCULAR CROSS-SECTION)

FACTOR $p = \frac{V_0^2}{V_0^2} = \frac{V^2}{V_0^2} = \frac{2\lambda_0}{A_0} \frac{z}{\lambda_0}$
 $\beta = \sqrt{1 - u_0^2}$

V_{x_2} vs X

$\frac{V_{x_2}}{V_0} (\beta \beta^2)$



$\beta = \frac{p - \lambda_0}{\lambda_0} = \frac{p - \lambda_0}{\lambda_0} \sqrt{1 - u_0^2}$

Figure 13: Wall Effect V_{x_2} Along Centerline $y = 0$ (See Walls).

| | | | | | | | | | | | | | | | | | | | | | | | | | | | | | | |
|-----|-----|-----|-----|-----|-----|-----|-----|-----|-----|-----|-----|-----|-----|-----|---|-----|-----|-----|-----|-----|-----|-----|-----|-----|-----|-----|-----|-----|-----|-----|
| 1.5 | 1.4 | 1.3 | 1.2 | 1.1 | 1.0 | 0.9 | 0.8 | 0.7 | 0.6 | 0.5 | 0.4 | 0.3 | 0.2 | 0.1 | 0 | 0.1 | 0.2 | 0.3 | 0.4 | 0.5 | 0.6 | 0.7 | 0.8 | 0.9 | 1.0 | 1.1 | 1.2 | 1.3 | 1.4 | 1.5 |
|-----|-----|-----|-----|-----|-----|-----|-----|-----|-----|-----|-----|-----|-----|-----|---|-----|-----|-----|-----|-----|-----|-----|-----|-----|-----|-----|-----|-----|-----|-----|

*

U

over
CONFIDENTIAL

400 358

20/4

ATI 173 032

(Copies obtainable from ASTIA-DSC)

WADC, Aeronautics Div., Wright-Patterson Air Force Base, O.
(WADC Technical Report 52-9)

unpub
(~~Confidential~~) Subsonic Flow Over a Body Between Porous Walls

Kassner, Rudolf R. Feb'52 34pp. table, diags, graphs

Flow, Two-dimensional

Aerodynamics (2)

~~Flow - Subsonic~~

Fluid Mechanics (9)

Flow - Velocity

Pressure distribution -

Measurement

Large Flow

CONFIDENTIAL

Pressure Measurement, Subsonic Flow

NTIS Auth: ASD ltr, 17 Sep 70

*U Auth: ltr fr WADC, W-9 APB dd 2 May 56
(WCLSW)*

AD-A800 091

nickel

9/29/05-